We are IntechOpen,
the world's leading publisher of
Open Access books
Built by scientists, for scientists

6,900
Open access books available

185,000
International authors and editors

200M
Downloads

154
Countries delivered to

Our authors are among the

TOP 1%
most cited scientists

12.2%
Contributors from top 500 universities

CLARIVATE ANALYTICS
BOOK CITATION INDEX
INDEXED

WEB OF SCIENCE™

Selection of our books indexed in the Book Citation Index
in Web of Science™ Core Collection (BKCI)

Interested in publishing with us?
Contact book.department@intechopen.com

Numbers displayed above are based on latest data collected.
For more information visit www.intechopen.com

Modeling of Full Electric and Hybrid Electric Vehicles

Ferdinando Luigi Mapelli and Davide Tarsitano

Additional information is available at the end of the chapter

1. Introduction

Full Electrical Vehicles (FEVs) and Hybrid Electrical Vehicles (HEVs) are vehicles with many electric components compared to conventional ones. In fact the power train consists of electrical machines, power electronics and electric energy storage system (battery, super capacitors) connected to mechanical components (transmissions, gear boxes and wheels) and, for HEV, to an Internal Combustion Engine (ICE). The approach for a new vehicle design has to be multidisciplinary in order to take into account the dynamic interaction among all the components of the vehicle and the power train itself. The vehicle designers in order to find the correct sizing of components, the best energy control strategy and to minimize the vehicle energy consumption need modeling and simulation since prototyping and testing are expensive and complex operations. Developing a simulation model with a sufficient level of accuracy for all the different components based on different physic domains (electric, mechanical, thermal, power electronic, electrochemical and control) is a challenge. Different commercial simulation tools have been proposed in literature and they are used by the automotive designer [1]. They have different level of detail and are based on different mathematical approaches. In paragraph 2 a general overview on different modeling approaches will be presented. In the following paragraphs the author approach, focused on the modeling of each component constituting a FEV or HEV will be detailed. The authors approach is general and is not based on vehicle oriented simulation tools. It represents a good compromise among model simplicity, flexibility, computational load and components detail representation. The chapter is organized as follows:

- paragraph 2 describes the different approaches that can be find in literature and introduced the proposed one;
- paragraphs 3 to 10 describe all the components modeling details in this order: battery, inverter, electric motor, vehicle mechanics, auxiliary load, ICE, thermal modeling;
- paragraph 11 presents different cases of study with simulation results where all the numerical models has been validated by means of experimental test performed by the authors.

2. FEV and HEV modeling

As shown in Figure 1, the whole vehicle power-train model is composed by many subsystems, connected in according to the energy and information physical exchanges. They represent the driver (pilot), the vehicle control system, the battery, the inverter, the Electrical Motor (EM), the mechanical transmission system, the auxiliary on board electrical loads, the vehicle dynamical model and for, HEVs and Plug-in Hybrid Electrical Vehicles (PHEVs), also an ICE and a fuel tank are considered. To correctly describe them, a multidisciplinary methodology analysis is required. Furthermore the design of a vehicle requires a complete system analysis including the control of the energy given from the on-board source, the optimization of the electric and electronic devices installed on the vehicle and the design of all the mechanical connection between the different power sources to reach the required performances. So, the complete simulation model has to describe the interactions between the system components, correctly representing the power flux exchanges, in order to help the designers during the study. For modeling each component, two different approaches can be used: an "equation-based" or a "map-based" mode [1]. In the first method, each subcomponent is defined by means of its quasi-static characteristic equations that have to be solved in order to obtain the output responses to the inputs. The main drawback is represented by the computational effort needed to resolve the model equations. Vice versa using a "map-based" approach each sub-model is represented by means of a set of look-up tables to numerically represents the set of working conditions. The map has to be defined by means of "off-line" calculation algorithm based on component model equation or collected experimental data. This approach implies a lighter computation load but is not parametric and requires an "off-line" map manipulation if a component parameter has to be changed. For the model developing process, an object-oriented causal approach can be adopted. In fact the complete model can be split into different subsystems. Each subsystem represents a component of the vehicle and contains the equations or the look-up table useful to describe its behavior. Consequently each object can be connected to the other objects by means of input and output variables. In this way, the equations describing each subsystem are not dependent by the external configuration, so every object is independent by the others and can be verified, modified, replaced without modify the equations of the rest of the model. At the same time, it is possible to define a "power flux" among the subsystems: every output variable of an object connected to an input signal of another creates a power flux from the first to the second subsystem ("causality approach"). This method has the advantage to realize a modular approach that allows to obtain different and complex configuration only rearranging the object connection.

A complete model can be composed connecting the objects according two different approaches: the "reverse approach" (also called "quasi-static approach" - see Figure 2) and the "forward approach" (also called "dynamic approach" - see Figure 3). Figure 2 and 3 show simplified models of a HEV, where V is the vehicle model, GB the gear box, PC the power converter, B the battery pack, FT the fuel tank, AL is the auxiliary loads block, v and a are respectively the vehicle's speed and acceleration, f is the vehicle traction force, Ω is the EM angular speed, T_{ICE} and T_{EM} are respectively the ICE and the EM torques, Ω_{ICE} is the ICE angular speed, f_c is the fuel consumption, I and V_s are the electrical motor current and voltage, i_{batt} and V_{batt} are the battery current and voltage, P_{InMot} is the power requested by the EM to the power converter, P_B is the total power requested to the battery that is obtained as a sum of the power requested by the power converter P_{InInv} and the
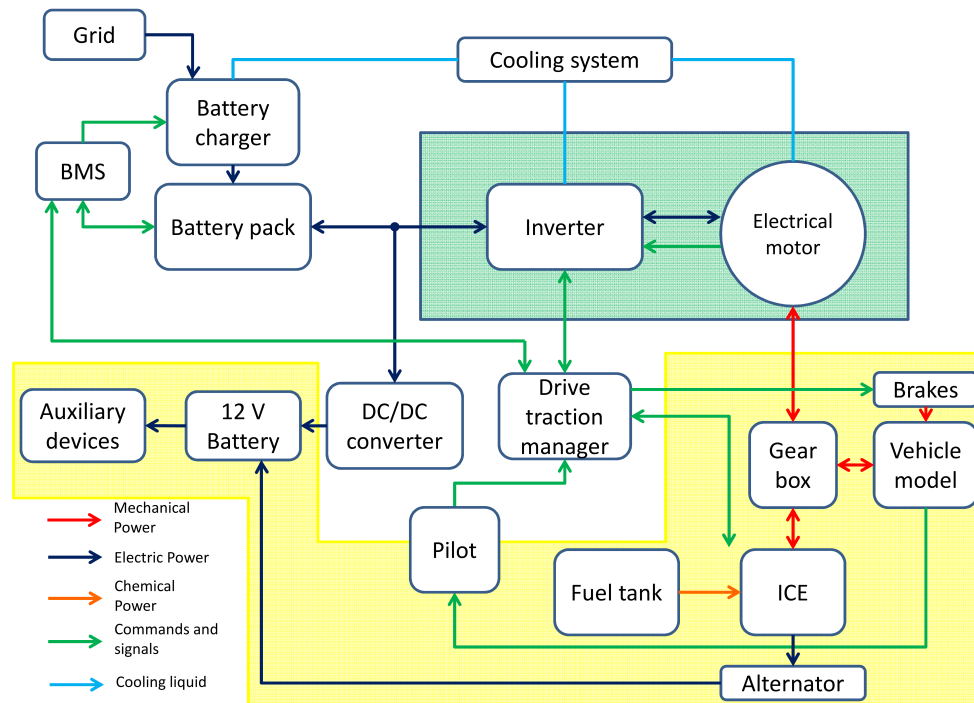
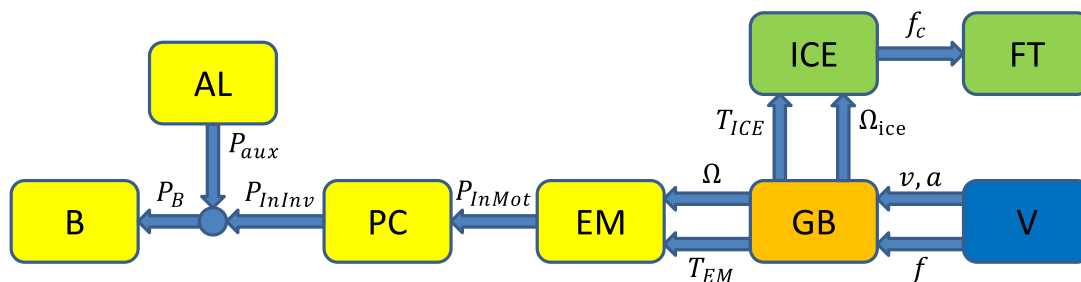**Figure 1.** Block diagram of a Plug-In HEV.

Figure 2. Example of HEV quasi-static modeling approach.

auxiliary loads P_{aux} ($P_B = P_{InInv} + P_{aux}$) and finally i_{aux} is the amount of current requested to the battery for auxiliary electrical loads. Quasi-static method use as input variables the desired speed and acceleration of the vehicle, hence the equations are solved starting from the V model and going back, block by block, to the B model. In the dynamic approach each subcomponent has interconnection variables with the previous and the next blocks. In this way each sub-model is strongly interleaved with the others and its behavior has influence on the total system. The second method requires a higher computational effort but is more accurate and has been applied by the authors in several cases [2–4]. In fact, using the first method, the information flux is unidirectional and the equation set is more simpler often only algebraic. This approach do not take into account the real response and constrain of power train component. On the contrary the dynamic approach produces also a response that runs
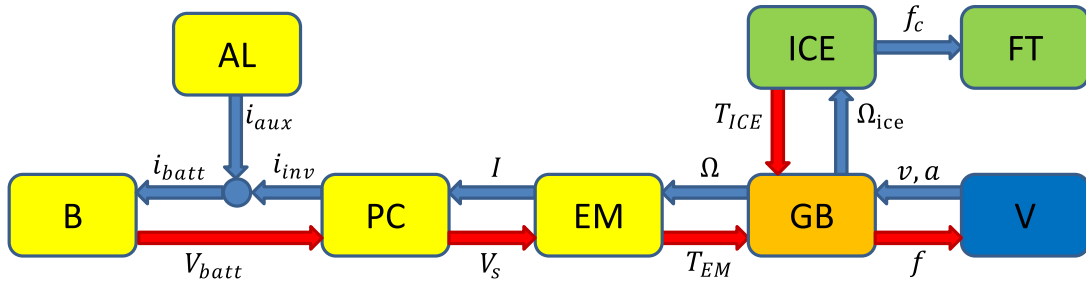
Figure 3. Example of HEV-dynamic modeling approach.

forward the complete model, influencing the output of the following sub-models. In this way, it is possible to study the total behavior including the physical limits of each component and, so, the simulation model is able to describe correctly both the single component and the overall performances of the system. For this method more complex equations (a few number of differential equation) or maps are needed. The following paragraphs describe component by component the proposed method which is based on a simplified dynamic forward approach that could be implemented using both equations or off-line computed look-up tables.

3. Battery modeling

In order to correctly simulate the behavior of a FEV, HEV or PHEV it is important to set up a battery model that evaluate the output voltage considering the State Of Charge (SOC) of the battery itself. Since a battery pack is obtained by a series connection of many cells (n_{cell}), it is quite usual to construct a numerical model considering one single cell. The total battery voltage V_{batt} is obtained using equation (1) assuming that all cells have an uniform behavior and where v_{el} is the voltage of a single cell.

$$V_{batt} = n_{cell} v_{el} \tag{1}$$

The battery model receives as input variables: the current i_{batt} required from the electrical drive model (inverter and electric motor) and the battery temperature ϑ computed by battery thermal model. The model gives as output variables: the battery pack voltage V_{batt}, the SOC and the power losses $P_{LossBatt}$. In order to simulate the battery behavior, instead of a complex electrochemical model, an Equivalent Circuit Model (ECM) can be chosen as a good compromise between accuracy and computational load. For example a first order Randles circuit (represented in Figure 4) can be adopted as dynamic model (see Paragraph 3.2); this model can be easily downgraded imposing $R_1 = 0$ in order to obtain a static model (see Paragraph 3.1). The circuit parameters can be deduced by experimental test or technical literature using the method described in [5].

Furthermore it is fundamental to calculate the battery SOC using equation (2) (where C_n is the rated capacity expressed in Ampere-Hours [Ah] and SOC_0 is the initial state of charge) to evaluate the amount of energy stored into the battery pack.
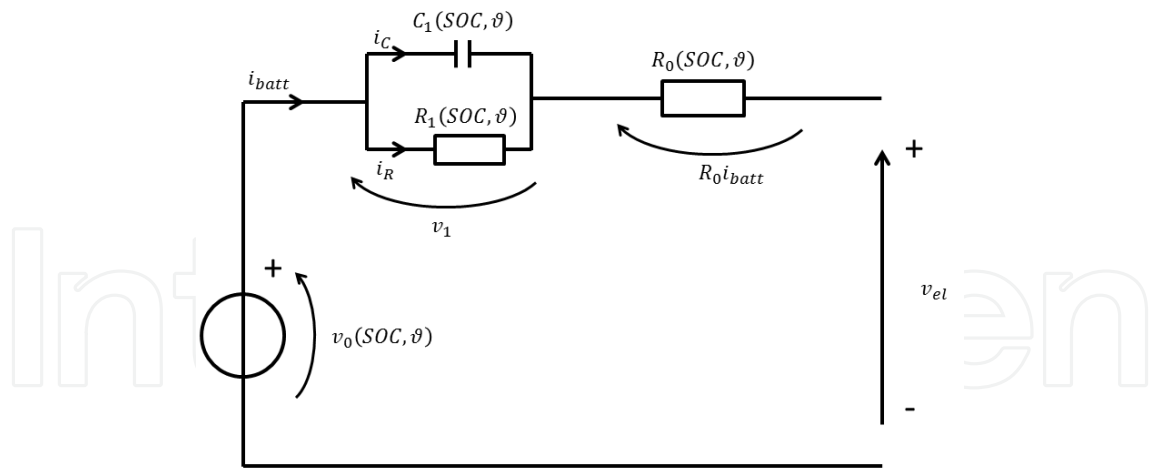
Figure 4. Randles electrodynamical model of a cell.

$$SOC(t) = SOC_0 - \int_0^t \frac{i_{batt}(t)}{3600 \cdot C_n} dt \qquad (2)$$

3.1. Static model of battery

Using the manufacturer charge and discharge charts and the data available for different temperature (reported as example in Figures 5-7), it is possible to reconstruct the map of $v_0(SOC, \vartheta)$ and of $R_0(SOC, \vartheta)$ and consequently to calculate $v_{el}(SOC, \vartheta)$ as reported in the static equation (3).

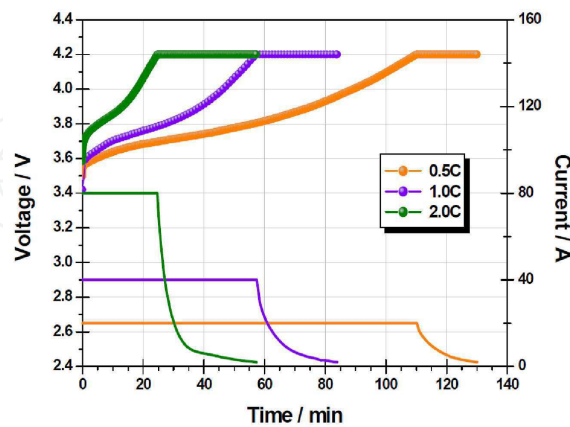$$v_{el}(SOC, \vartheta) = v_0(SOC, \vartheta) - R_0(SOC, \vartheta)i_{batt} \qquad (3)$$

Figure 5. Charging chart for different C-Rates.

A further simplification is to consider the temperature ϑ constant and consequently to calculate and to represent on a map the v_{el} as reported in Figure 8, as a function of the battery SOC and the battery current i_{batt}.
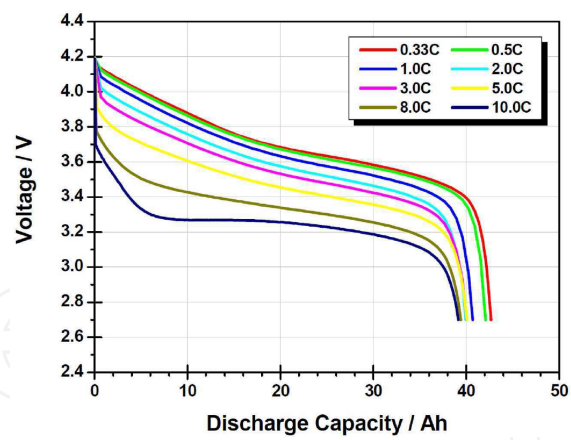
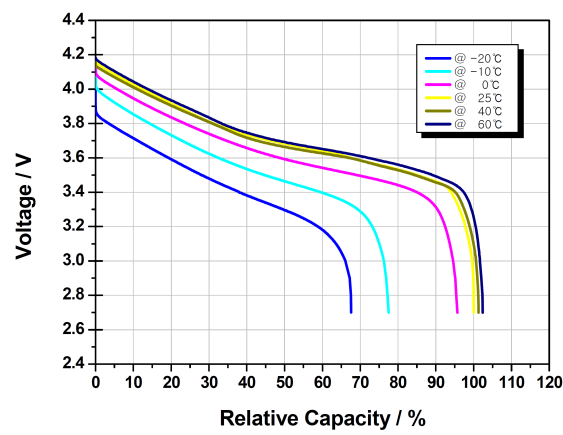**Figure 6.** Discharge chart for different C-Rates.

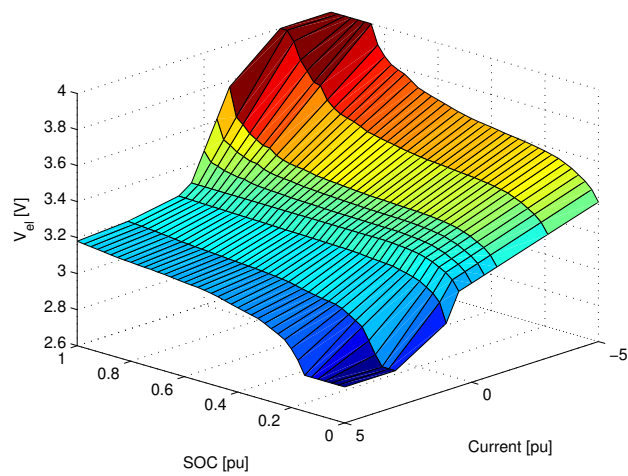**Figure 7.** 1C discharge chart for different temperatures.

Figure 8. Battery voltage map.

3.2. Dynamical model of battery

Since batteries for traction application are used under heavy dynamic condition with suddenly variation of the supplied current i_{batt}, the static model can not be adopted for all the cases of study where dynamic is fundamental (for example control analysis). Different type

of ECM have been developed for simulating battery voltage v_{el} where more that one *RC* block are used in order to obtain a Ordinary Differential Equation (ODE) of order n and a parasitic parallel branch is added to the ECM to simulate the self discharge phenomenon. Since the main objective is not to simulate all the battery details but the global vehicle behavior a single *RC* circuit for an enough accurate model can be adopted, as reported in Figure 4.

In order to have good simulation results a fine tuning of the dynamic ECM parameters has to be done. A good procedure for parameter identification, considering also thermal effects, is reported in [5].

It possible to solve the circuit considering the cell voltage v_{el}, as reported in equation (4)[1], where the splitting of the total current i_{batt} into the capacitor C_1 and into the resistor R_1 is considered ad reported in equation (5) and the no load voltage v_0 is SOC dependant.

$$v_{el} = v_0 - R_0 i_{batt} - v_1 \tag{4}$$

$$\begin{cases} i_{batt} = i_c + i_r \\ i_c = C_1 \dfrac{dv_1}{dt} \\ i_r = \dfrac{v_1}{R_1} \end{cases} \tag{5}$$

Finally, substituting i_{batt} obtained from equation (5) in equation (4), is possible to obtain the final dynamic equation of the cell voltage, as reported in equation (6).

$$\frac{dv_1}{dt} = \frac{1}{R_0 C_1} \left(v_0(SOC) - v_{el} - v_0(SOC) \left(1 + \frac{R_0}{R_1} \right) \right) \tag{6}$$

4. Inverter modeling

Different methods are available in the scientific literature in order to evaluate power electronic converter losses [6, 7] and to obtain a consequent energetic model. The most simple approach is to consider the power converter as an equivalent resistive load where the inner power losses are proportional to the square of the flowing current. Since in the most cases the power converter assumes the three phase inverter topology the power losses expression can be formalized as reported in (7), where R_{Inv} is the inverter equivalent resistance and I is the Root Mean Square (RMS) inverter output phase current (that corresponds to the EM phase input RMS current).

$$P_{LossInv} = 3 \cdot R_{Inv} \cdot I^2 \tag{7}$$

---

[1] In equation (4) (5) (6) where: it has been neglected the dependency of the circuital parameters from battery SOC and temperature ϑ.

The inverter input power can be calculated adding the inverter losses $P_{LossInv}$ to the motor input power P_{InMot} that correspond to the inverter output power P_{OutInv} (equation (8)).

$$P_{InInv} = P_{LossInv} + P_{InMot} = P_{LossInv} + P_{OutInv} \qquad (8)$$

A more detailed approach can be described if the simulation model adopted includes the control and inverter modulator details: an instant circuit losses model can be also implemented [6]. The losses are computed considering the basic inverter cell composed of an Insulated Gate Bipolar Transistor (IGBT) and a diode. The inverter is formed by six basic cells divided into 3 arms as reported in Figure 9.

The instantaneous losses of a basic cell p_{cell} can be evaluated using equation (9) where: p_{swT} are transistor switching losses, E_{on} and E_{off} are turn-on and turn off energy, f_s is the inverter switching frequency, E_{recD} and p_{recD} are the recovery diode energy and power losses, v_{ce} and v_{ak} are respectively the transistor and diode forward voltage drop, i_c and i_f are the transistor and diode direct current ad p_{fwT} and p_{fwD} are transistor and diode conduction forward losses. The total inverter instantaneous losses are reported in (10). For the IGBT and diode the typical current Vs voltage curves and the switch on/off energy losses Vs current charts are shown in Figure 11, 12 and 13.

These curves can be simplified as shown in equation (11) where all the parameters (A_{fwT}, B_{fwT}, A_{fwD}, B_{fwD}, B_{onT}, C_{onT}, B_{offT}, C_{offT}, B_{recD}, C_{recD}) can be deduced from the semiconductor device technical data sheet [8, 9]. Equation (12) can be obtained substituting equation (11) into the (10). These equations express the instantaneous losses p_{inv} as a function of semiconductor devices current.

$$\begin{cases} p_{fwT} = v_{ce}(i_c) \cdot i_c \\ p_{fwD} = v_{ak}(i_f) \cdot i_f \\ p_{swT} = [E_{on}(i_c) + E_{off}(i_c)] f_s \\ p_{recD} = E_{recD}(i_d) \cdot f_s \\ p_{cell} = p_{swT} + p_{recD} + p_{fwT} + p_{fwD} \end{cases} \qquad (9)$$

$$p_{inv} = 6 \cdot p_{cell} \qquad (10)$$

$$\begin{cases} v_{ce}(i_c) = A_{fwT} + B_{fwT} i_c \\ v_{ak}(i_f) = A_{fwD} + B_{fwD} i_f \\ E_{onT}(i_c) = B_{onT} i_c + C_{onT} i_c^2 \\ E_{offT}(i_c) = B_{offT} i_c + C_{offT} i_c^2 \\ E_{recD}(i_f) = B_{recD} i_f + C_{recD} i_f^2 \end{cases} \qquad (11)$$
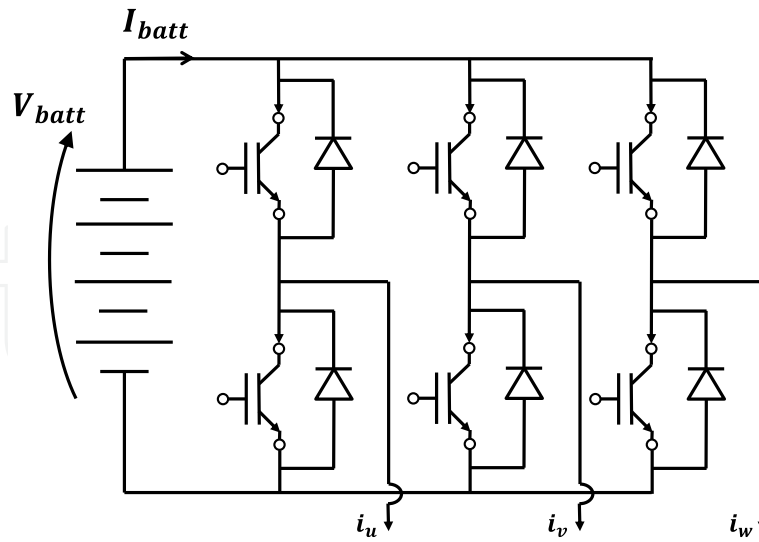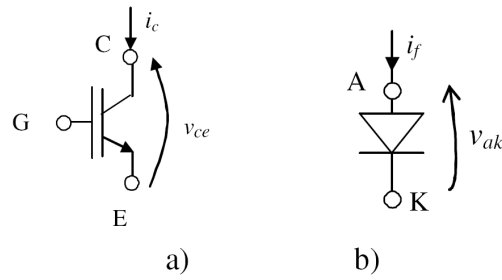
Figure 9. Battery fed three phase inverter

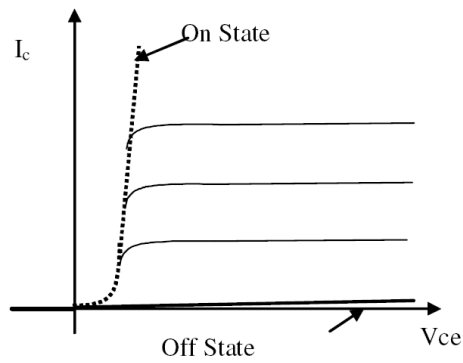**Figure 10.** Symbols and definitions for Igbt a) and Diode b).

Figure 11. IGBT current Vs voltage diagram.

$$\begin{cases} p_{fwT}(i_c) = A_{fwT}i_c + B_{fwT}i_c^2 \\ p_{fwD}(i_f) = A_{fwD}i_f + B_{fwD}i_f^2 \\ p_{swT}(i_c) = (B_{onT}i_c + C_{onT}i_c^2)f_s + (B_{offT}i_c + C_{offT}i_c^2)f_s \\ p_{recD}(i_f) = (B_{recD}i_f + C_{recD}i_f^2)f_s \end{cases} \quad (12)$$
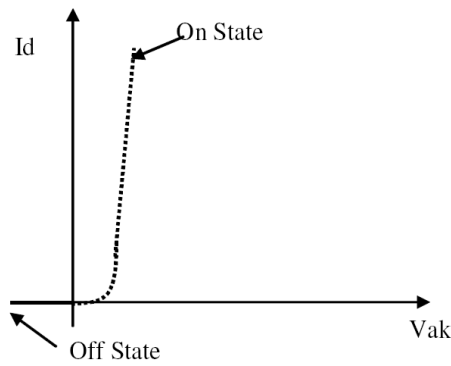
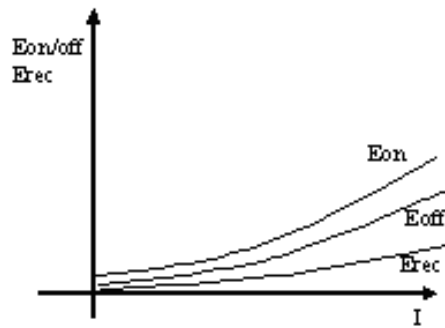**Figure 12.** Diode current Vs voltage diagram.

Figure 13. IGBT/Diode switching energy vs current.

The instantaneous inverter losses expressions (10) need, in order to be evaluated, the calculation of the instantaneous alternate three-phase motor current. This fact implies that the simulation model has to be solved with a very short integration step with a consequent high computation load and large simulation time. For FEV and HEV power train modeling purpose such time details and accuracy is not needed but the exact losses calculation is necessary on a larger time scale. An average approach on an alternate quantities period can be adopted. In this way a larger time step is enough and the RMS value of alternate voltage and current can be used. In this method the losses calculation accuracy is assured and very fast phenomena (evolution during a AC current period T) are neglected. This approximation is sufficient for vehicle power train modeling and for energy and power flow analysis. Assuming sinusoidal time dependency for current, as reported in equation (13) where: I_M is the maximum current value, $\omega = 2\pi/T$ is the current angular frequency and φ is the phase angle between motor voltage and current, substituting the (13) into equation (12) and assuming that $i = i_c = i_f$, the instantaneous inverter losses with explicit time dependence can be obtained. Averaging the losses on an Alternating Current (AC) variables period T is possible to obtain the losses mean value [10]. The average relationships are obtained as reported in equation (14) where: T_s is the IGBT switching period, T_{dead} is the dead time between high and low side IGBT switch on operation and $\cos\varphi$ is the motor power factor. The total PWM operation cell average losses P_{PWM} are the all terms sum, while the total averaged inverter losses P_{invPWM} are reported in equation (15).

$$i(t) = I_M cos(\omega t - \varphi) \tag{13}$$

$$
\begin{cases}
P_{fwT} = \left(\frac{1}{2} - \frac{T_{dead}}{T_s} \right) \left(\frac{A_{fwT}}{\pi} I_M + \frac{B_{fwT}}{4} I_M^2 \right) + m \cos \varphi \left(\frac{A_{fwT}}{8} I_M + \frac{B_{fwT}}{3\pi} I_M^2 \right) \\
P_{fwD} = \left(\frac{1}{2} - \frac{T_{dead}}{T_s} \right) \left(\frac{A_{fwD}}{\pi} I_M + \frac{B_{fwD}}{4} I_M^2 \right) - m \cos \varphi \left(\frac{A_{fwD}}{8} I_M + \frac{B_{fwD}}{3\pi} I_M^2 \right) \\
P_{onT} = f_s I_M \left(\frac{B_{onT}}{\pi} + \frac{C_{onT}}{4} I_M \right) \\
P_{offT} = f_s I_M \left(\frac{B_{offT}}{\pi} + \frac{C_{offT}}{4} I_M \right) \\
P_{recD} = f_s I_M \left(\frac{B_{recD}}{\pi} + \frac{C_{recD}}{4} I_M \right) \\
P_{PWM} = P_{onT} + P_{offT} + P_{fwT} + P_{fwD} + P_{recD}
\end{cases}
\tag{14}
$$

$$P_{invPWM} = 6 \cdot P_{PWM} \tag{15}$$

Since the inverter sub-model receives as input V_s, I, $\cos \varphi$ and ω, previously evaluated by the electric motor model, and V_{batt} (the available battery voltage) it can calculate the current required to the battery i_{inv} and the total inverter losses P_{PWM}. The sequence of equations to be solved is reported as follows:

1. total power supplied to the motor calculation: $P_{InMot} = \sqrt{3} V_s I cos\varphi$;

2. inverter AC phase current max. value calculation: $I_M = \sqrt{2} I$;

3. inverter PWM amplitude modulation index calculation: $m = \sqrt{2} V_s / V_{batt}$;

4. total inverter averaged losses P_{invPWM} calculation by means of equation (14) and (15);

5. total inverter input power calculation: $P_{InInv} = P_{InMot} + P_{invPWM}$;

6. inverter input current calculation: $i_{inv} = P_{InInv} / V_{batt}$.

5. Electrical motor modeling

The most adopted motors for FEV and HEV are AC induction motors and AC Permanent Synchronous Magnets Motor (PMSM) regulated by means of a field oriented control or direct torque control. In this section the models of both motors will be presented using a phase vector approach [11, 12] and considering the motor field oriented controlled. For both motor models it is possible to define the input and output variables as follows:

•   input: required torque T_{ref}, instantaneous rotating mechanical speed Ω, battery voltage V_{batt};

- output: torque T_{EM}, RMS phase current I, line to line voltage V_s, power factor angle φ, total losses $P_{LossMot}$, Motor input (P_{InMot}) and output power (P_m), electrical frequency f and angular frequency $\omega = 2\pi f$.

For FEV and HEV power train modeling and simulation a complete motor model including the detailed electromechanical dynamic is not required; it is better to use a steady state model that consider the controlled motor including all the energetic phenomena (power losses calculation). The proposed model include also limits and constrains due to the motor power supplier, which is based on batteries and inverter, such as maximum deliverable voltage, power and current.

5.1. Induction motor

For the induction motor the steady state equations [13] are reported in equation (16) where $\bar{V}_s$, $\bar{I}_s$ and $\bar{\psi}_r$ are respectively stator voltage, stator current and rotor flux phasors, R_s, R_r, M, L_k are respectively stator resistance, rotor resistance, mutual inductance and total leakage inductance, n is the pole pairs number, T_{EM} is the torque , $\bar{I}_m$ is the magnetizing current phasor, $\bar{I}_r$ is rotor or torque current phasor, Ω is the mechanical angular speed, x is the relative rotor slip speed, ω is the AC variable angular frequency and j the imaginary unit. Equation (16) can be represented by means of the equivalent circuit reported in Figure 14.

The three phase motor is modeled using a "rational" approach that correspond to have a "single phase'equivalent" model also for energetic relations and torque expression [13]. In fact the amplitude of current phasor $\bar{I}_s$ and the stator voltage phasor $\bar{V}_s$ are related to the RMS phase current I and voltage V by means of equation (17). The induction motor model includes also equation (18) where ψ_{rn} is the induction motor rated flux, ω_n is the rated motor angular frequency, P_{Cu} and P_{Fe} represent respectively the copper and iron losses and Q_{InMot} is the motor reactive input power. Equation (18) allows to calculate all the power terms and stator quantities to be used as inputs for inverter and battery model.

$$\begin{cases} \bar{V}_s = R_s\bar{I}_s + j\omega L_{ks}\bar{I}_s + j\omega M\bar{I}_m \\ 0 = -\dfrac{R_r}{x} \cdot \bar{I}_r + j\omega M\bar{I}_m \\ \bar{I}_s = \bar{I}_r + \bar{I}_m \\ \bar{\psi}_r = M\bar{I}_m \\ x = \dfrac{\omega - n\Omega}{\omega} \\ T = nM I_m I_r = n\psi_r I_r \end{cases} \tag{16}$$

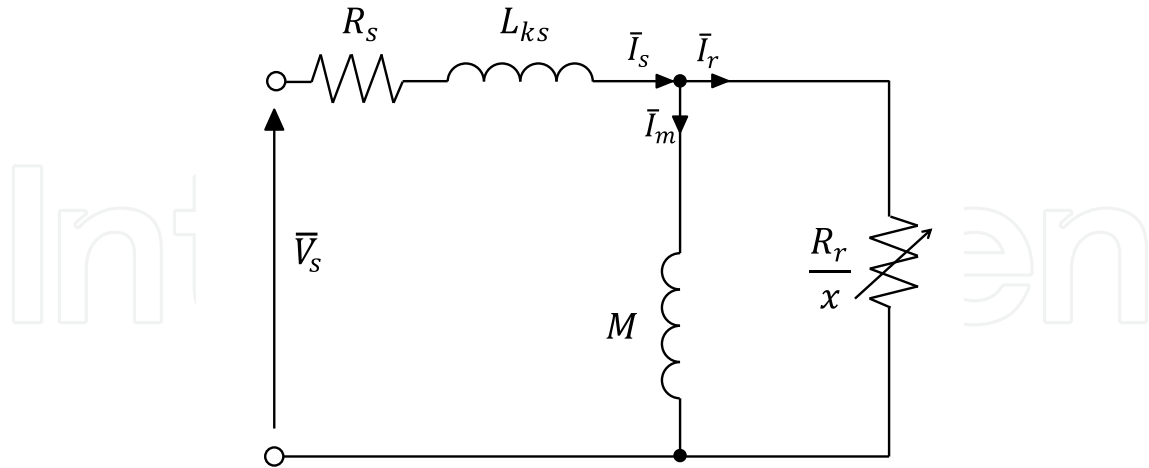$$\left\{ V_s = V \cdot \sqrt{3} I_s = I \cdot \sqrt{3} \right. \tag{17}$$

Figure 14. Induction motor steady-state equivalent circuit.

$$
\begin{cases}
P_{Cu} = R_s I_s^2 + R_r I_r^2 \\[2mm]
P_{Fe} = P_{Fen} \dfrac{\omega}{\omega_n} \dfrac{\psi_r^2}{\psi_{rn}^2} \\[2mm]
P_{LossMot} = P_{Cu} + P_{Fe} \\[2mm]
P_m = T\Omega \\[2mm]
P_{InMot} = P_{LossMot} + P_m \\[2mm]
Q_{InMot} = \omega M I_m^2 + \omega L_{ks} I_s^2 \\[2mm]
\varphi = atan \left(\dfrac{Q_{InMot}}{P_{InMot}} \right)
\end{cases}
\tag{18}
$$

Equations (16) and (18) have to be solved together with equation (19) that define the rotor flux value as function of the rotating speed Ω and of the rated speed Ω_n. Equation (19) represents the field weakening condition for the induction motor. Furthermore it is also necessary to control that the torque request T_{ref} does not exceed the maximum motor torque T_{refMax} and the consequent power request $(T_{ref} \cdot \Omega)$ does not exceed the motor power limit P_{motMax} (see equation (20)).

$$
\begin{cases}
\psi_r = \psi_{rn} & \text{if} \quad \Omega < \Omega_n \\[2mm]
\psi_r = \psi_{rn} \dfrac{\Omega_n}{\Omega} & \text{if} \quad \Omega > \Omega_n
\end{cases}
\tag{19}
$$

$$
\begin{cases}
T_{ref} = T_{refMax} & \text{if} \quad T_{ref} > T_{refMax} \\[2mm]
T_{ref} = P_{motMax}/\Omega & \text{if} \quad T_{ref} \cdot \Omega > P_{motMax}
\end{cases}
\tag{20}
$$

Moreover the global electrical drive limits verification has to be taken into account in order to avoid that the requested operating point do not correspond to an allowed condition. The three conditions to consider are:

1. maximum RMS input current I_{max} that is related to the inverter current limit (as reported in equation (21));
2. maximum motor voltage limit V_{sMax} that correspond to the maximum deliverable inverter voltage for a given battery voltage (as reported in equation (22));
3. the maximum motor input power limit P_{inMax} that is related to the maximum battery deliverable power (as reported in equation (23)).

These conditions have to be verified and imposed after the calculation of equations (20), (19), (16) and (18).

$$I = \frac{I_s}{\sqrt{3}} < I_{max} \tag{21}$$

$$V_s < V_{sMax} \quad \text{then} \quad V_{sMax} = \frac{V_{batt}}{\sqrt{2}} \tag{22}$$

$$P_{InMot} < P_{inMax} \tag{23}$$

The proposed model can be used for off-line map calculation, that can be included in the simulation model, or calculated directly on-line during the numerical simulation process. The calculus procedure for induction motor can be summarized as follows:

1. verify if the torque request T_{ref} is compliant with absolute motor torque and power limit otherwise saturate T_{ref} using the (20);

2. solve the field weakening conditions (19);

3. solve the (16), (18) using as input variables $T_{EM} = T_{ref}$ and Ω;

4. verify the (21), (22) and (23), in order to impose the motor, inverter and battery limitations;

5. if the condition (21) is not respected reduce T_{ref}, go back to step 3 and iterate;

6. if the condition (22) is not respected reduce ψ_r, go back to step 3 and iterate;

7. if the condition (23) is not respected reduce T_{ref}, go back to step 3 and iterate.

5.2. Permanent magnets synchronous brushless motor

For the Permanent Synchronous Magnets Motor the steady state equation [11] are reported in equation (24) where: V_d and V_q are the stator voltage phasor $\bar{V}_s$ components ($\bar{V}_s = V_d + jV_q$), I_d and I_q are the stator current phasor $\bar{I}_s$ components ($\bar{I}_s = I_d + jI_q$), R_s is the stator resistance, L_s is the stator synchronous inductance, ψ_m is the permanent magnet flux phasor. The other symbols, T_{EM}, Ω, ω and n assume the same meaning that ones indicated in the induction motor description.

Equation (24) has to be solved, also in this case, together with equations (25) and (26). Similarly to the induction motor a pre-process operation on torque request T_{ref} has to be implemented in order to impose the respect of torque and power motor limit. Furthermore the field weakening condition have to be imposed to the motor. It consists in setting the correct value of I_d current [12] by means of equation (27). In fact the current I_d can be maintained equal to zero in the constant torque/flux region and has to be imposed negative in the field weakening zone. Finally also the limit input conditions have to be taken into account using the same equations of the induction motor ((21), (22) and (23)).

$$\begin{cases} V_d = R_s I_d - \omega L_s I_q \\ V_q = R_s I_q + \omega L_s I_d + \psi_m \omega \\ T_{EM} = n \psi_m I_q \\ \Omega = \dfrac{\omega}{n} \end{cases} \tag{24}$$

$$\begin{cases} P_{Cu} = R_s I_d^2 + R_s I_q^2 \\ P_{Fe} = P_{Fen} \dfrac{\omega}{\omega_n} \\ P_m = T_{EM} \Omega \\ P_{LossMot} = P_{Cu} + P_{Fe} \\ P_{InMot} = P_m + P_{LossMot} \end{cases} \tag{25}$$

$$\begin{cases} I_s = \sqrt{I_d^2 + I_q^2} \\ V_s = \sqrt{V_d^2 + V_q^2} \\ Q_{InMot} = V_q I_d - V_d I_q \\ \varphi = atan\left(\dfrac{Q_{InMot}}{P_{InMot}}\right) \end{cases} \tag{26}$$

$$\begin{cases} \psi_s = \psi_m & \text{if} \quad \Omega < \Omega_n \\ \psi_s = \psi_m \dfrac{\Omega_n}{\Omega} & \text{if} \quad \Omega > \Omega_n \\ Id = \dfrac{\psi_s - \psi_m}{L_s} \end{cases} \tag{27}$$

Also in this case the model can be used both for off-line map calculation and on-line numerical simulation process.

The calculus procedure for PMSM can be summarized as follows:

1. verify if the torque request T_{ref} is compliant with absolute motor torque and power limit otherwise saturate T_{ref} using equation (20);
2. solve the field weakening conditions (equation (27));
3. solve equations (24), (25) and (26) using as input $T_{EM} = T_{ref}$ and Ω;
4. verify equations (21),(22) and (23), in order to impose the motor, inverter and battery limitation;
5. if the condition (21) is not respected reduce T_{ref}, go back to step 3 and iterate;
6. if the condition (22) is not respected reduce ψ_s, go back to step 2 and iterate;
7. if the condition (23) is not respected reduce T_{ref}, go back to step 3 and iterate.

In Figure 15 is reported, as example, an efficiency map of a $65kW$ peak power PMSM obtained by means of the proposed model, for a 2500 kg mass FEV. The per unit efficiency η_{EM} can be calculated using equation (28).
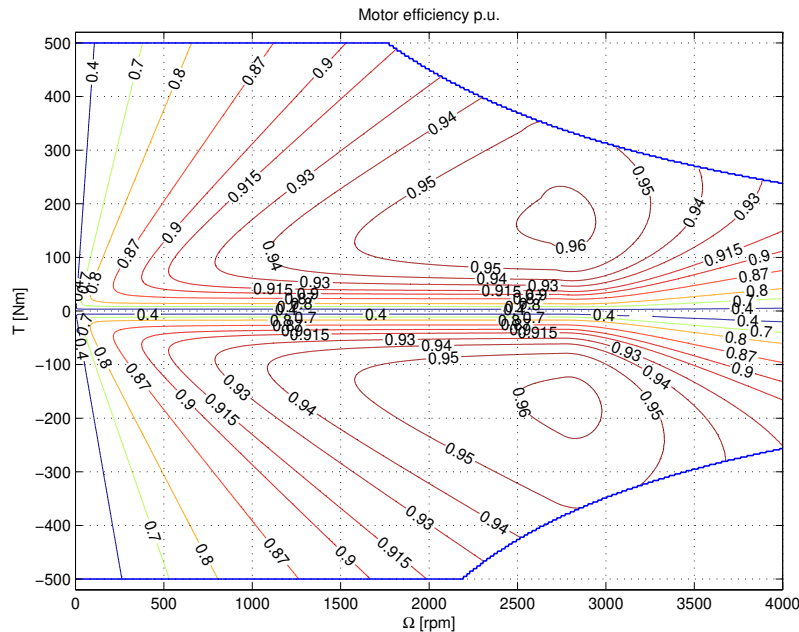
$$\eta_{EM} = \frac{P_m}{P_{InMot}} \tag{28}$$

Figure 15. Efficiency map for a PMSM as function of torque and speed.

6. Vehicle longitudinal dynamic modeling

In order to reconstruct the energetic power flow between FEV and HEV components a simple vehcile longitudinal dynamic model has to be considered. In this paragraph the model will be described considering the most general case constituted by an HEV; the model of a FEV can be simply deducted neglecting all the ICE contributions. This model receives as input the torque given by the ICE T_{ICE} and by the EM T_{EM} coming from the respective simulation models and the gear ratio of the mechanical gearbox coming from the pilot model and calculate the vehicle speed $v(t)$ and distance covered $s(t)$.

As first it is necessary to evaluate the total torque at the wheels T_w as sum of the EM torque reported at the wheel T_{EMw} with the ICE torque reported at the wheel T_{ICEw}. For this all the reduction ratios and the efficiencies of the transmission chain have to be considered, as reported in equations (29) and (30), which are specialized for traction condition (29) and for braking condition (30). In these equations τ_{EM} and $\eta_{\tau EM}$ are respectively the reduction ratio of the EM and its efficiency, τ_{ICE} and $\eta_{\tau ICE}$ are respectively the reduction ratio of the ICE and its efficiency, τ_{diff} and η_{diff} are respectively the differential reduction ratio and its efficiency.

$$\begin{cases} T_{EMw} = T_{EM} \cdot \tau_{EM} \cdot \tau_{diff} \cdot \eta_{\tau EM} \cdot \eta_{diff} \\ T_{ICEw} = T_{ICE} \cdot \tau_{ICE} \cdot \tau_{diff} \cdot \eta_{\tau ICE} \cdot \eta_{diff} \end{cases} \tag{29}$$

$$\begin{cases} T_{EMw} = \dfrac{T_{EM} \cdot \tau_{EM} \cdot \tau_{diff}}{\eta_{diff} \cdot \eta_{\tau EM}} \\ T_{ICEw} = \dfrac{T_{ICE} \cdot \tau_{ICE} \cdot \tau_{diff}}{\eta_{\tau ICE} \cdot \eta_{diff}} \end{cases} \tag{30}$$

Usually for an HEV the ICE has a mechanical gearbox with $5 \div 7$ fixed reduction ratios and the EM has an unique fixed reduction ration. For this reason the longitudinal dynamic model receive as input from the driver model the correct gear that has to be considered.

In order to define the longitudinal equivalent dynamic equation it is also necessary to introduce all the resistance forces acting on the vehicle, as reported in equation (31), where: m is the total mass of the vehicle, g is the gravitational acceleration, f_v is the rolling resistance coefficient, ρ is the air density, C_x is the aerodynamic penetration coefficient, S is the total frontal area of the vehicle , α is the slope of the road.

$$F_{res} = m \cdot g \cdot f_v + \frac{1}{2}\rho C_x S v(t)^2 + m \cdot g \cdot \sin\alpha \tag{31}$$

Finally it is possible to evaluate the vehicle acceleration a, as reported in equation (32), where r_w is the radius of the vehicle wheels, m^* represents the equivalent mass of the rotating part of the vehicle (wheels, rotor, shaft)[2].

$$\begin{cases} f = \dfrac{T_w}{r_w} \\ a = \dfrac{T_w/r_w - F_{res}}{(m + m^*)} \end{cases} \tag{32}$$

Using vehicle longitudinal acceleration a from equation (32), it is possible to obtain vehicle speed and position.

$$\begin{cases} v(t) = \int_0^t a(t)dt \\ s(t) = \int_0^t v(t)dt \end{cases} \tag{33}$$

Finally the EM and the ICE speed are obtained as described in equation (34).

$$\begin{cases} \Omega = \dfrac{v(t)\tau_{EM}\tau_{diff}}{r_w} \\ \Omega_{ICE} = \dfrac{v(t)\tau_{ICE}\tau_{diff}}{r_w} \end{cases} \tag{34}$$

7. Auxiliary loads model

7.1. Auxiliary electrical loads

In order to correctly estimate the energy consumption on a FEV it is important to consider all the auxiliary electrical loads that the traction battery has to fed.

Particularly the low voltage loads (12 or $24V_{dc}$), represented for example by light, circulating pump, fan and control units, have to be estimated considering an adequate average value of power consumption during the trip. The energy for these loads is usually delivered by the traction battery through a DC/DC converter. The battery current i_{aux} can be calculated with equation (35) using the power consumption P_{aux} of electrical auxiliary loads, the battery voltage V_{batt} from the battery model and the efficiency of the DC/DC converter $\eta_{DC/DC}$.

---

[2] As example the equivalent mass representing the EM inertia referred to the vehicle can be evaluated considering the following equation.

$$m^*_{EM} = \frac{J_{EM}\tau_{EM}^2\tau_{diff}^2}{r_w^2}$$

$$i_{aux} = \frac{P_{aux}}{V_{batt}\eta_{DC/DC}} \tag{35}$$

7.2. Pumps

On HEVs and FEVs are usually installed liquid cooled electrical traction devices, in particular motor and inverter. For this reason auxiliary circulation pumps are needed in order to guarantee an adequate heat exchange between the components and the cooling fluid.

It is possible to estimate the hydraulic power P_{hy} required for the pump using equation (36), where ρ is the fluid density, Q the volumetric flow rate, g the gravity constant, h is the total head of the hydraulic circuit and h_l is an equivalent of hydraulic losses expressed in meter of water column. Usually the term h_l, that is responsible of a pressure drop Δp_l, is preponderant with respect to h and strictly depends from the design of the cooling circuit into the component.

$$P_{hy} = \rho Q g(h + h_l) = \rho Q g \left(h + \frac{\Delta p_l}{\rho g}\right) \tag{36}$$

At last, using a pump efficiency (η_{pump}) given by the manufacturer, it is possible to evaluate the electrical power requirement on the auxiliary load using equation (37).

$$P_{el} = \frac{P_{hy}}{\eta_{pump}} \tag{37}$$

8. ICE modeling

Since an accurate model of thermal combustion process require a wide knowledge of ICE design (i.e. intake and exhaust geometry, geometry of cylinder, spark position and timing, ...) a map based model is sufficient in order to estimate the engine fuel consumption and efficiency on drive cycle with a time scale of hundred of seconds.

The structure of the ICE model receive as input the torque request from the energy management control and the ICE speed from the longitudinal dynamic model and gives as output the effective torque T_{ICE}, the instantaneous volumetric fuel consumption f_c and the amount of CO_2 produced. A global structure of the model is represented in Figure 16.

The maps inserted into the ICE block can be obtained directly from the engine manufacturer; otherwise they can be obtained through experimentally tests using an engine test bench or directly on the vehicle using the Controller Area Network (CAN) information. An example of torque and fuel consumption map referred to the vehicle reported in paragraph 11.1 is reported in Figures 17 and 18.

For the volume L of fuel present in the tank equation (38) can be used, where L_0 represents the initial volume condition.
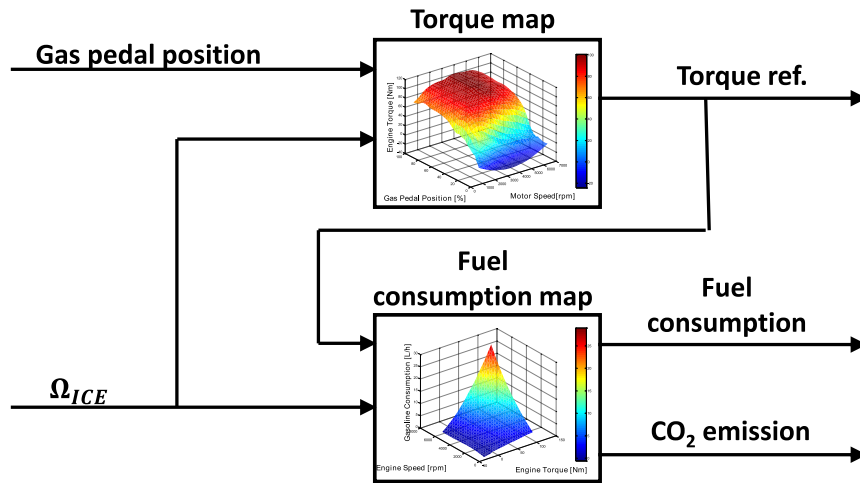
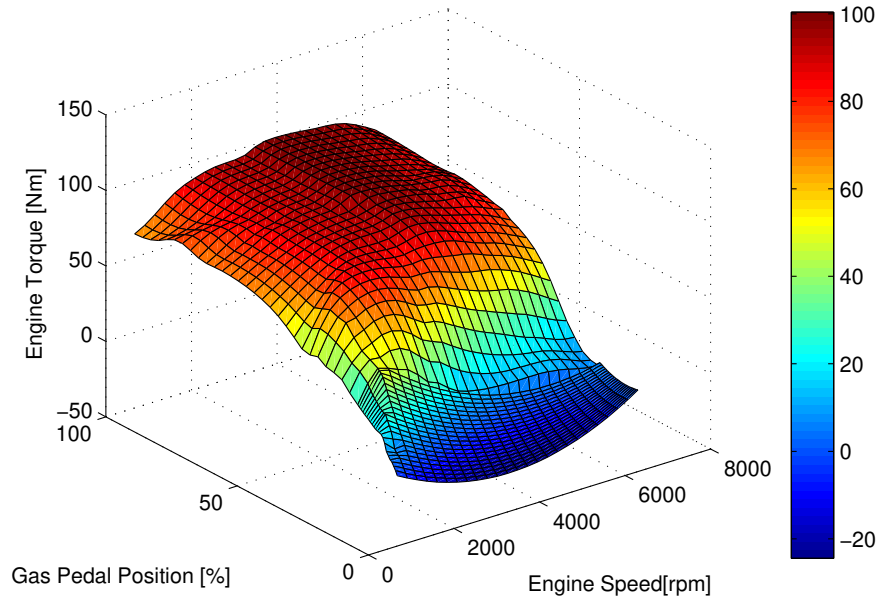**Figure 16.** Block scheme for ICE

Figure 17. Engine torque map.

$$L = L_0 - \int_0^t f_c dt \tag{38}$$

Other approach for ICE modeling can be settled up using theoretical approaches as reported in [14].

Finally a rough estimation of the CO_2 emission can be established using equation (39), in which ρ_C is the average content of carbon in gasoline, M_{mCO_2} is the molar mass of CO_2, M_{mC} is the carbon molar mass and φ is a coefficient for incomplete combustion.
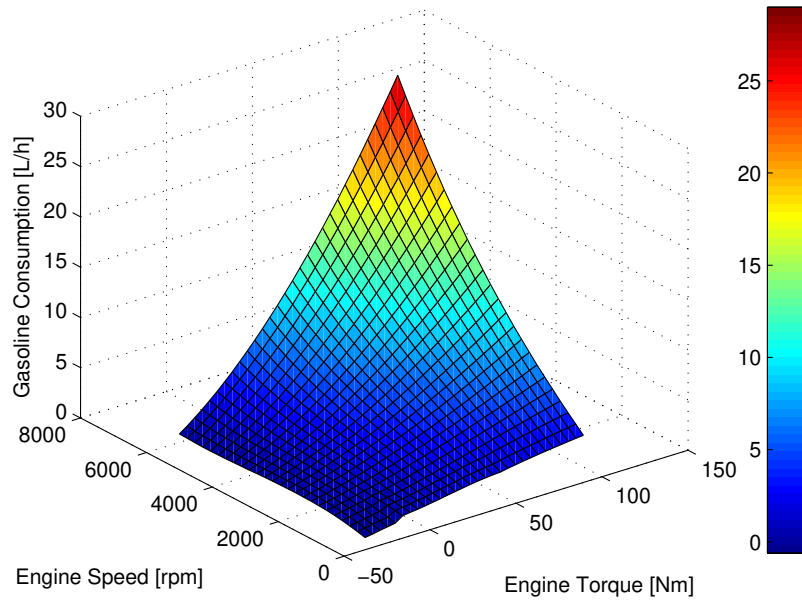
Figure 18. Engine fuel consumption map.

$$CO_2 = f_c \cdot \rho_C \cdot \frac{M_{mCO_2}}{M_{mC}} \cdot \varphi \tag{39}$$

9. Thermal modeling

The different FEV and HEV components and subsystems can be modeled including a simple thermal equivalent network where each component is considered as an homogeneous body. The chosen model is a first order lumped parameters thermal network [15] where: P_{lc} are the total component power losses, C_c is the total thermal capacity, R_c is the total thermal resistance that represent all the transfer heating phenomena (conduction, convention and radiation heat transfer), $\Delta\vartheta_c = \vartheta_c - \vartheta_{mean}$ is the temperature difference between the component inner temperature ϑ_c and the reference temperature ϑ_{mean}. The first order ODE is reported in equation (40) and the equivalent network is reported in Figure 19.

$$\begin{cases} P_{lc} = \dfrac{\Delta\vartheta_c}{R_c} + C_c \cdot \dfrac{d\Delta\vartheta_c}{dt} \\ \vartheta_c = \vartheta_{mean} + \Delta\vartheta_c \end{cases} \tag{40}$$

If the component is natural-air cooled the reference temperature ϑ_{mean} is equal to the ambient temperature ϑ_{amb}. Otherwise, if a forced-air cooling system is adopted, the equivalent thermal resistance R_c assumes different values as a function of the cooling fan status. Therefore if the cooling fan is running the $R_c = R_{cON}$ that corresponds to a lower value than $R_c = R_{cOFF}$ when the fan is stopped. A more sophisticated model can relate the R_c parameter as a function of the fan speed.
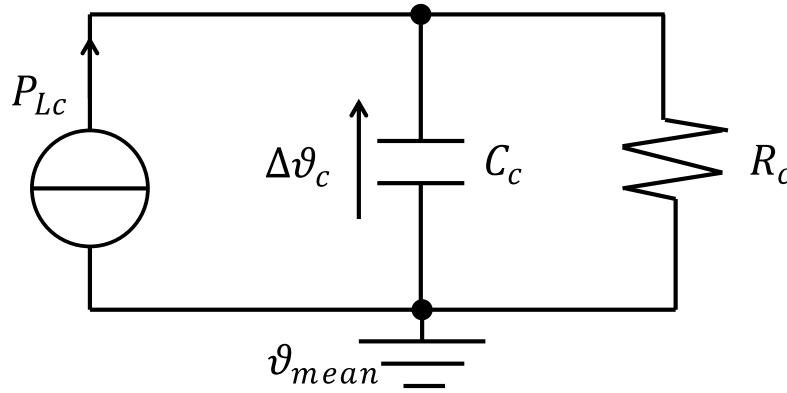
Figure 19. General component thermal model.

A FEV and HEV liquid-cooling system is often adopted especially for ICE, EM and inverter. The cooling system is based on an hydraulic circuit where a cooling fluid (usually a 50 % mix of water and glicole) is pumped into the components to be cooled and in a liquid-air heat exchanger, wich is usually forced air cooled by means of cooling fans. For these situations the thermal model of the liquid-based cooling system is to be considered too. Also in this case a first order ODE reported in equation (41) can be used. The equivalent circuit is reported in Figure 20 where: P_{ltot} are the sum of the total losses of the components that are liquid-cooled, R_{liq} is the equivalent variable thermal resistance of the liquid-air heat exchanger, C_{liq} is the liquid cooling system equivalent thermal capacity, ϑ_{liq} is the average liquid temperature in the cooling liquid circuit and $\Delta\vartheta_{liq}$ is the temperature difference between liquid and ambient.

In this case the reference temperature ϑ_{mean} for the component thermal model of Figure 19 has to be taken equal to the liquid average temperature ($\vartheta_{mean} = \vartheta_{liq}$). The equivalent liquid cooling system thermal resistance R_{liq} is a time-variant parameter since it depends on the air-liquid heat exchanger cooling fan status. For example can "switch" between two values if the fan is ON/OFF controlled (R_{liqON} when fan is on and R_{liqOFF} when is off).

$$\begin{cases} P_{ltot} = \dfrac{\Delta\vartheta_{liq}}{R_{liq}} + C_{liq} \cdot \dfrac{d\Delta\vartheta_{liq}}{dt} \\ \vartheta_{liq} = \vartheta_{amb} + \Delta\vartheta_{liq} \end{cases} \tag{41}$$

10. Driver and energy management control

The model receives as input the drive cycle that the vehicle has to execute; this reference is given to a pilot model that gives as output a signal representative of driver torque request; the pilot model acts as a speed closed loop that compares the required speed to the instantaneous one coming from the vehicle longitudinal dynamic model. Considering the vehicle structure (hybrid or full electric) and the hybrid control logic, the traction manager control splits the pilot request of torque between the ICE, the EM and the mechanical brakes, as reported in Figure 21. In this block, through torque vs speed curves, the required torques, both for the electrical and for the ICE motor, is saturated to the limit values.
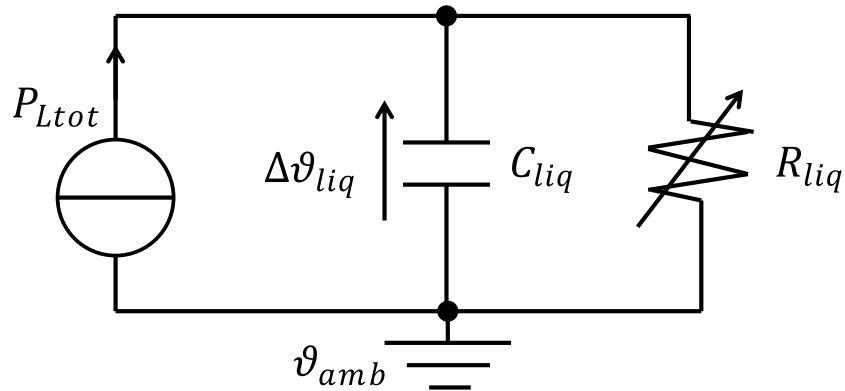
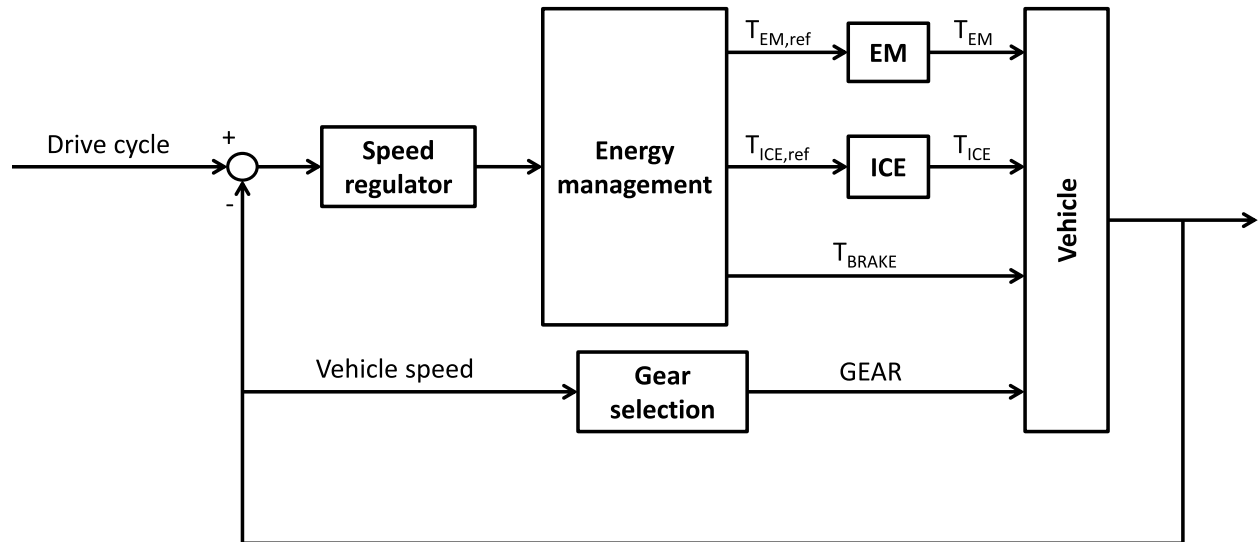**Figure 20.** Radiator dynamic thermal model.

Figure 21. Driver and energy management control block scheme.

At last for the ICE gearbox a simple algorithm to set the correct ratio has to be implemented. The algorithm increase the gear if the ICE speed Ω_{ICE} exceed a certain threshold and decrease the gear if the speed Ω_{ICE} is below a different threshold. It is important to introduce an hysteresis zone on the speed Ω_{ICE} in order to avoid continuous gear shift.

11. Examples

In the current section some results compared with experimental data will be presented.

11.1. B segment car

In this section a B segment car will be considered; this car, originally propelled only with an ICE, has been transformed in a PHEV capable to run as a FEV up to 70 km/h and to cover a driving range of about 40km. The main data of the vehicle are reported in Table 1.

Vehicle data			
Vehicle		**Internal Combustion Engine**	
Vehicle mass	1100kg	Fuel	Gasoline
Gearbox ratios	3.90 2.15 1.48 1.12 0.92	Max Torque	102Nm
Final ratio	4.071	Max Power	50kW
Wheel radius	0.27m	Total Displacement	1200cc

Table 1. Vehicle data.

11.1.1. Electrical power train simulation

First of all the validation of the vehicle behavior when run as a FEV will be presented. For this purpose it has been requested to the model to follow the same drive cycle executed using prototypal vehicle during experimental tests; this drive cycle is reproduced in Figure 22.

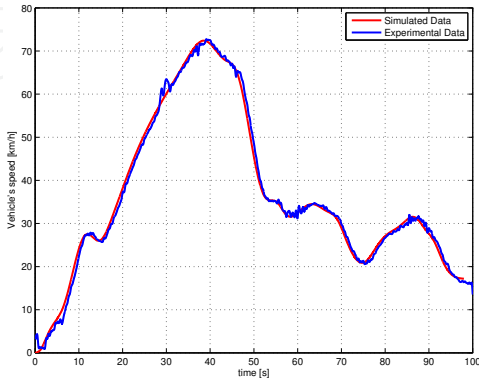| Electrical traction system data					
Battery		**Inverter**		**Motor**	
Element type	Li-Ion	V_{DC}	$80-400V$	Type	Induction
Number of elements	60	Typology	FOC	Peak Power	30kW
Rated Capacity	50Ah	Rated Current	234A	Rated Speed	2950rpm
Rated Voltage	222V	Max Current	352A	Rated Voltage	105V
Min. Voltage	252V	Aux Supply	12V_{DC}	Rated Current	70A
Max. Voltage	192V	Cooling	Water	No Load Curr.	33.6A
Total Energy	11,1kWh			Pole number	4
Max. Power	30kW			Cooling	Water

Table 2. Electrical traction system data.

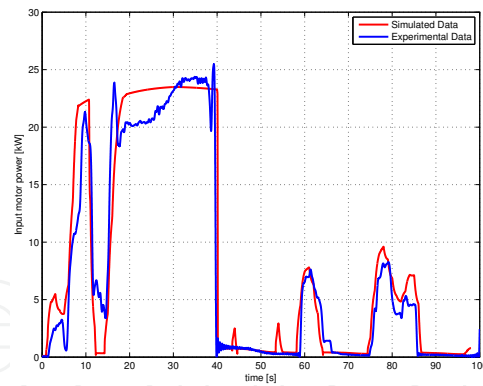**Figure 22.** Electrical drive cylce.

Figure 23. Electric motor power.

Using the cycle represented in Figure 22 it is possible to validate the battery model in terms of total voltage v_{batt} and in terms of current i_{batt}. The comparison between the model simulation results and the experimental data is shown in Figures 26 and 27. In the over mentioned figures it is also reported the energy consumption E evaluated through the acquired data and through the output of the vehicle's model. The comparison shows a good correspondence between the simulation and experimental data; as consequence the kilometric energy consumption is also well estimated by the model. Furthermore it is possible to validate the electrical motor model by numerical-experimental comparison performed considering the output power, as reported in Figure 23, the phase current and line to line voltage, as reported respectively in Figures 24 and 25.
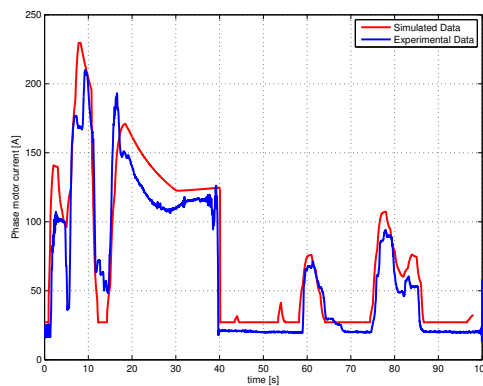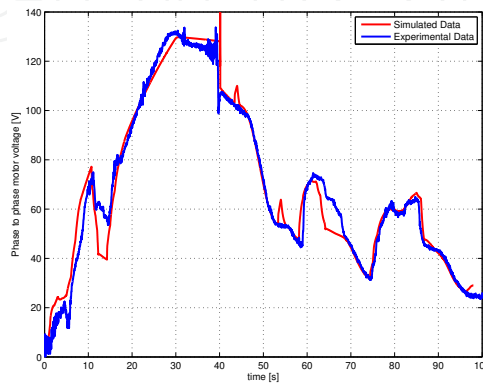

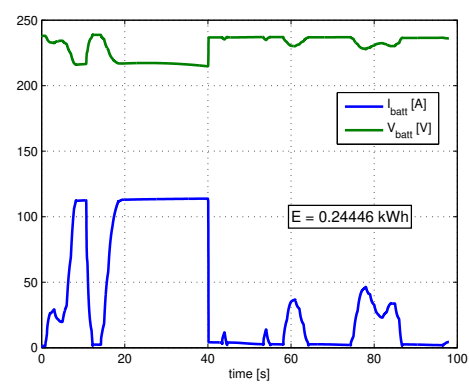**Figure 24.** Motor phase current.

Figure 25. Motor phase to phase voltage.
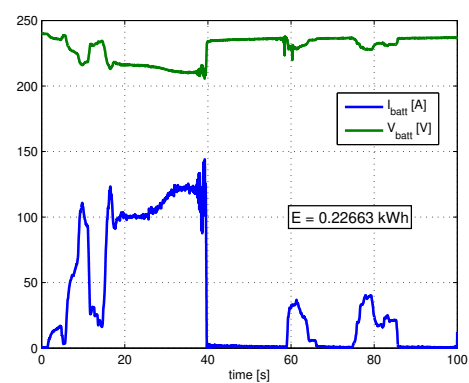
Figure 26. Simulated battery data.

Figure 27. Real battery data.

11.1.2. Hybrid power train simulation

At last it has been implemented a Start&Stop strategy on the prototypal vehicle. This very simple strategy ask to the electrical drive traction system to propel the vehicle up to a speed threshold set to 32 km/h; above this speed threshold the vehicle is propelled by the ICE motor.
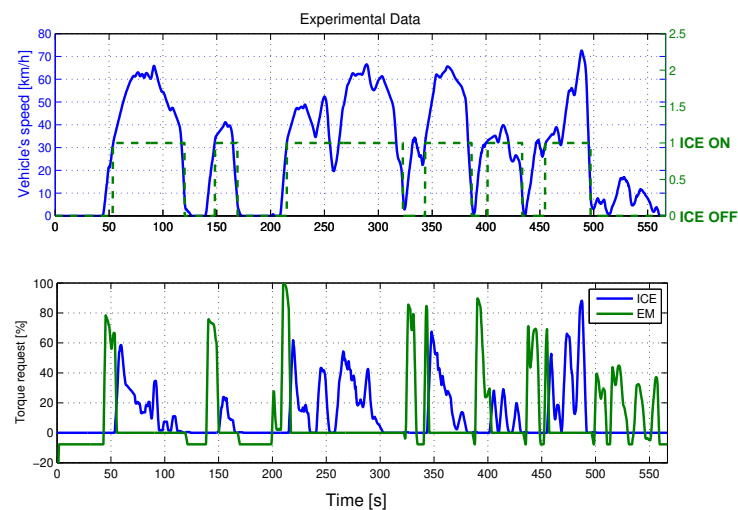

Figure 28. Drive cycle with superimposed the ICE status

In the upper part of Figure 28 it is shown the drive cycle used to validate the model in the Start&Stop mode and in the lower part it is shown the torque request repartition between the electrical motor and the ICE motor.

Finally in Figures 29 and 30 it is reported the comparison of experimental data and simulation results obtained using the drive cycle and the strategy reported in Figures 28.
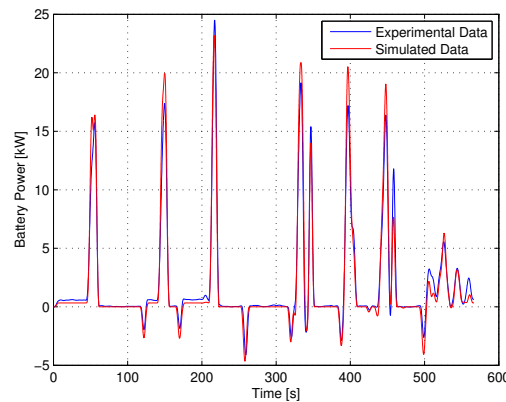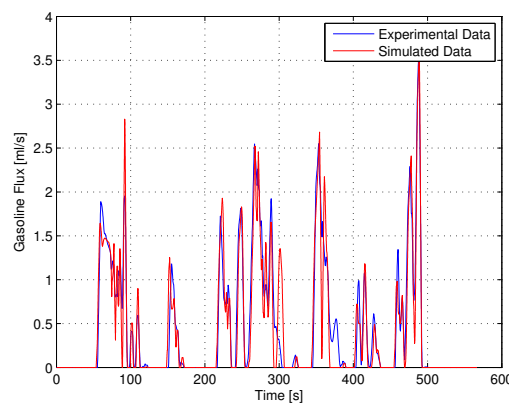

Figure 29. Battery power.

Figure 30. ICE gasoline flux.

11.2. Commercial vehicle

In this section a full electric commercial van will be considered. Its main characteristics are reported in Table 3.

As done for the previously described PHEV it has been requested to the simulation model to cover the same driving cycle executed by the prototypal vehicle (Figure 31).

Finally in Figures 32 and 33 are reported some comparison between simulated data and experimental ones; in particular Figure 32 refers to the EM torque and Figure 33 refers to the total battery current i_{batt}.

Full Electric truck data			
Vehicle		**Battery**	
Vehicle mass	$2500kg$	Element Type	Li-Ion
Final ratios	3.75	Number of elements	68
Wheel radius	0.325	Rated Capacity	$90Ah$
Max weight	$3500kg$	Rated Voltage	217
Inverter		**Electrical Motor**	
V_{DC}	$80 - 400V$	Type	Induction
Typology	FOC	Peak Power	$60kW$
Rated Current	$240A_{RMS}$	Rated Speed	$2400rpm$
Max Current	$350A_{RMS}$	Rated Voltage	$115V$
Aux Supply	$12V_{DC}$	Rated Current	$200A$
Cooling	Water	No Load Curr.	$95A$
		Pole number	4

Table 3. Electrical traction system data.
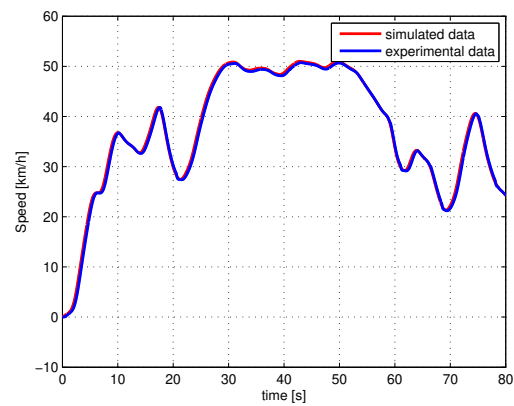

Figure 31. Drive cycle for the full electric commercial vehicle.
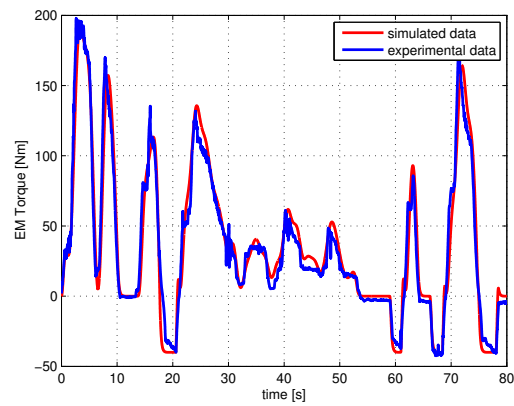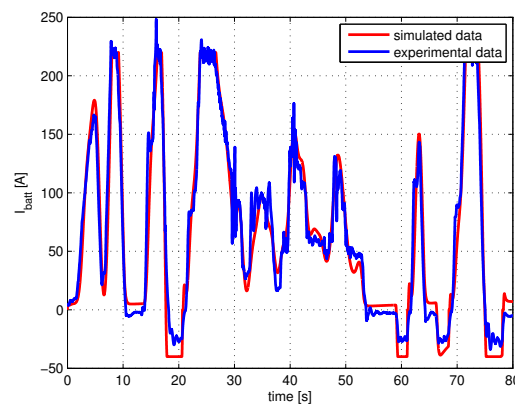

Figure 32. EM torque.

Figure 33. Total battery current i_{batt}.

12. List of Acronyms

HEV Hybrid Electrical Vehicle

RMS Root Mean Square

PHEV Plug-in Hybrid Electrical Vehicle

FEV Full Electrical Vehicle

SOC State Of Charge

IGBT Insulated Gate Bipolar Transistor

EM Electrical Motor

ICE Internal Combustion Engine

CAN Controller Area Network

ECM Equivalent Circuit Model

ODE Ordinary Differential Equation

FOC Field Oriented Control

AC Alternating Current

PMSM Permanent Synchronous Magnets Motor

PWM Pulse Width Modulation

Acknowledgements

Author details

Ferdinando Luigi Mapelli and Davide Tarsitano

Mechanical Department, Politecnico di Milano, Milan, Italy

References

[1] D. W. Gao, C. , Mi, and A. Emadi. Modeling and simulation of electric and hybrid vehicles. *Proceedings of the IEEE*, 95(4):729–745, 2007.

[2] F. Cheli, F.L. Mapelli, R. Manigrasso, and D. Tarsitano. Full energetic model of a plug-in hybrid electrical vehicle. In *SPEEDAM 2008 - International Symposium on Power Electronics, Electrical Drives, Automation and Motion*, pages 733–738, Ischia, 2008.

[3] F. L. Mapelli, D. Tarsitano, and M. Mauri. Plug-in hybrid electric vehicle: Modeling, prototype realization, and inverter losses reduction analysis. *IEEE Transactions on Industrial Electronics*, 57:598–607, 2010.

[4] F.L. Mapelli, D. Tarsitano, and A. Stefano. Plug-in hybrid electrical commercial vehicle: Modeling and prototype realization. In *2012 IEEE International Electric Vehicle Conference, IEVC 2012*, Greenville, SC, 2012.

[5] T. Huria, M. Ceraolo, J. Gazzarri, and R. Jackey. High fidelity electrical model with thermal dependence for characterization and simulation of high power lithium battery cells. In *2012 IEEE International Electric Vehicle Conference, IEVC 2012*, Greenville, SC, 2012.

[6] A. Fratta and F. Scapino. Modeling inverter losses for circuit simulation. In *Conference of 2004 IEEE 35th Annual Power Electronics Specialists Conference, PESC04;*, volume 6, pages 4479–4485, Aachen, 2004.

[7] R. Manigrasso and F.L. Mapelli. Design and modelling of asynchronous traction drives fed by limited power source. In *Conference of 2005 IEEE Vehicle Power and Propulsion Conference, VPPC*, volume 2005, pages 522–529, Chicago, IL, 2005.

[8] http://www.infineon.com/cms/en/product/index.html

[9] http://www.infineon.com/cms/en/product/index.html

[10] R. Manigrasso and F.L. Mapelli. Design and modelling of asynchronous traction drives fed by limited power source. In *IEEE Vehicle Power and Propulsion Conference, VPPC*, volume 2005, pages 522–529, Chicago, IL, 2005.

[11] P. Vas. *Electrical machines and drives: a space-vector theory approach*. Clarendon Press, 1992.

[12] P. Vas. *Vector Control of AC Machines*. Clarendon Press, 1990.

[13] M. Mauri, F.L. Mapelli, and D. Tarsitano. A reduced losses field oriented control for plug-in hybrid electrical vehicle. In *19th International Conference on Electrical Machines, ICEM 2010*, Rome, 2010.

[14] G. Rizzoni, L. Guzzella, and B.M. Baumann. Unified modeling of hybrid electric vehicle drivetrains. *IEEE/ASME Transactions on Mechatronics*, 4(3):246–257, 1999.

[15] M. M. Rathore and R. Kapuno. *Engineering Heat Transfer*. Jones & Bartlett Publishers, 2010.